

# Temporal and spatial variability of rainfall over Greece

Y. Markonis\*, S. C. Batelis, Y. Dimakos, E. Moschou and D. Koutsoyiannis

Department of Water Resources and Environmental Engineering, Faculty of Civil Engineering,  
National Technical University of Athens, Heroon Polytechniou 5, GR 157 80 Zographou, Greece

\*Corresponding author: imarkonis@itia.ntua.gr – tel.: +30 210 7722838

## ABSTRACT

Recent studies have showed that there is a significant decrease in rainfall over Greece during the last half of the pervious century, following an overall decrease of the precipitation at the eastern Mediterranean. However, during the last decade an increase in rainfall was observed in most regions of the country, contrary to the general circulation climate models forecasts. An updated high-resolution dataset of monthly sums and annual daily maxima records derived from 136 stations during the period 1940 – 2012 allowed us to present some new evidence for the observed change and its statistical significance. The statistical framework used to determine the significance of the slopes in annual rain was not limited to the time independency assumption (Mann-Kendall test), but we also investigated the effect of short- and long-term persistence through Monte Carlo simulation. Our findings show that (a) change occurs in different scales; most regions show a decline since 1950, an increase since 1980 and remain stable during the last 15 years, (b) the significance of the observed decline is highly dependent to the statistical assumptions used; there are indications that the Mann-Kendall test may be the least suitable method and (c) change in time is strongly linked with the change in space; for scales below 40 years relatively close regions may develop even opposite trends, while in larger scales change is more uniform.

**Keywords:** climate variability, climate networks, eastern Mediterranean, Greece, Hurst, long term persistence, rainfall trends

# 1. INTRODUCTION

Our study area is Greece, a mid-latitude country located at the south-easternmost part of the European continent. The two most prominent geographical features are the proximity to the Mediterranean Sea and the complex orography with abrupt elevation changes. The Pindus mountain range stretches along the western part of the country in a northwestern-southeastern direction, dividing it in two halves. The larger plains can be found in the central and northern regions of the country, while the majority of the wetlands are situated at the western part (Figure 1A).

Greece's topography and the surrounding sea have a strong impact to the local climate leading to considerable spatial variability. Nine different climatic types according to Köppen classification can be found, with the Cs class being dominant, i.e. the Mediterranean climatic type, but also including Cf, Df and Ds classes in smaller proportions (Malliaros 2013). The overall temporal pattern exhibits strong seasonality, dividing the hydrological year into a wet (late autumn, winter and early spring) and a drier (mainly summer) period. In terms of spatial variability, higher annual rain is observed to the western part of Greece reaching as high as 1900 mm per year, while dry conditions prevail over the south-eastern part with anhydrous summers and annual rainfall sums, that may fall below 350 mm (this study).

This is due to the combined effect of the orographic factor and the large scale atmospheric circulation over the Euro-Mediterranean area, which is characterized by strong complexity (Bolle 2003, Lionello 2012). During the wet period the high elevation of the Pindus mountain range blocks the cyclones which are mainly generated at the Gulf of Genoa and move eastwards (Dünkeloh and Jacobeit 2003, Kostopoulou and Jones 2007). It should be noted that the cyclonic weather types are associated to over 90% of the total precipitation and hence the rainfall regime is strongly connected to the atmospheric pressure patterns (Maheras and Anagnostopoulou 2003, Maheras et al. 2004, Xoplaki et al. 2004, Kostopoulou and Jones 2007).

In larger scale, winter rainfall in the Eastern Mediterranean region was found to be linked with many teleconnection patterns such as the North Atlantic Oscillation (Hurrell 1995, Cullen and Demenocal 2000, Eshel and Farrell 2000, Dünkeloh and Jacobeit 2003), the east Atlantic – west Russia pattern (Krichak and Alpert 2005), the Arctic Oscillation (Dünkeloh and Jacobeit 2003) and the Mediterranean Oscillation (Kutiel et al. 1996, Dünkeloh and Jacobeit 2003). Rainfall over Greece follows a similar correlation scheme, which becomes stronger during the winter months and milder during the dry period (Xoplaki et al. 2000, Maheras and Anagnostopoulou 2003, Feidas et al. 2007). However, the most dominant teleconnection pattern affecting winter precipitation over Greece is the recently-identified Eastern-Mediterranean Pattern (EMP), which appears as a dipole between northeastern Atlantic and eastern Mediterranean (Hatzaki et al. 2007, 2009).

Earlier analysis of rainfall data over Greece suggests that there is a steady decline in annual rain since 1950 especially during winter months (Xoplaki et al. 2000, Maheras and Anagnostopoulou 2003, Maheras et al. 2004, Feidas et al. 2007, Kambezidis et al. 2010). Similar results have been presented for the neighboring regions and the Mediterranean Sea in general, most of them presenting a significant decrease in annual rainfall (González-Hidalgo et al. 2001, Xoplaki et al. 2004, Cannarozzo et al. 2006, Norrant and Douguédroit 2006, Partal and Kahya 2006, Nastos 2011, Philandras et al. 2011). The general circulation climate models (GCMs) also point towards the same direction, predicting a gradual aridification of the Mediterranean region not only in their forecasts,

but also in their hindcasts as the IPCC reports and the references within suggest (Houghton 1996, Griggs and Noguer 2002, Solomon 2007, Stocker et al. 2013).

Our study is based on monthly data and daily maxima per year from 136 stations being active during the period 1940-2012 (Figure 1C-4), which offer a good representation of rainfall variability over Greece. Regions that share statistical properties (see Section 2.2) are identified and the correlations between them are investigated. Furthermore, since the most recent studies cover the years between 1950 and 2000 and do not include the last decade, we provide new evidence on the quantification of change and its significance. To this end we estimate slope significance stochastically with Monte Carlo simulation under three different hypotheses instead of following the Mann-Kendal non-parametric test approach (Mann 1945, Kendall 1948), which can lead to overestimation of the exceedance probability due to the presence of short-term or long-term persistence (Hamed and Ramachandra Rao 1998, Cohn and Lins 2005).

## 2. DATA AND METHODS

### 2.1 Data

The original dataset consisted of 38 records acquired from the Hellenic National Meteorological Service (HNMS) and 146 records from the Special Secretariat of Water (SSW) summing to a total of 186 records of monthly precipitation and daily maximum precipitation of each month, mainly distributed in the continental Greece. Some preliminary criteria were applied to ensure data consistency and low missing value content.

An upper threshold of 1000 m for the elevation was taken to reduce the orographic effect; in addition it should be noted that the majority of the remaining stations are located below 400 m (Table 1). The homogeneity of the stations was also examined in correlation basis and a few dubious cases were removed, e.g. single stations non-correlated with their adjacent ones. The missing-value limit was set at the 20% of record length only for monthly sums, since daily maxima were not studied in terms of slopes. Finally, monthly records with total time length below 40 years were omitted, as well as records with less than 20 complete years of monthly data (240 months). The former restriction was crucial in order to study the change in slopes, while the latter resulted in a better aggregation to the annual scale. After the application of these criteria, the dataset consisted of 29 records from HNMS and 107 from SSW summing up to a total of 136 records.

Two time scales were investigated, the monthly sums and the annual daily maxima, i.e. the maximum value of daily rain per year derived from the maximum daily precipitation of each month. The period examined covered the years 1940 – 2012 (Figure 1C-4), but the majority of stations started operating after 1950 (Figures 1B-1 and 1C-1). Missing values are quite lower than preliminary threshold of 20%, as for the two thirds of the stations the ratio of missing values versus record length falls below 5% (Figure 1C-2). In terms of absolute numbers record lengths range between 400 and 800 months, with the majority lying between 500 and 750 (mean close to 670; approximately 55 years). During the period between 1953 and 2009, the number of stations without any missing monthly values or daily maxima is above 50 for each individual year (Figure 1C-4). A final examination of the ratio of maximum consecutive missing values versus record length was performed to ensure that there are no significant gaps in data that could bias the estimation of slopes. As it can be seen in Figure 1C-5 the majority of the records were below 0.05, or 3 years.

Annual daily maxima present a different picture, with higher missing values ratios (Figure 1B-2) and shorter record lengths (Figure 1B-3; mean close to 39 values). This is due to the fact that only years without any missing values were used to determine each annual daily maximum and inevitably restricts their study to the presentation of their statistical properties in space and not their evolution in time (i.e. slopes).

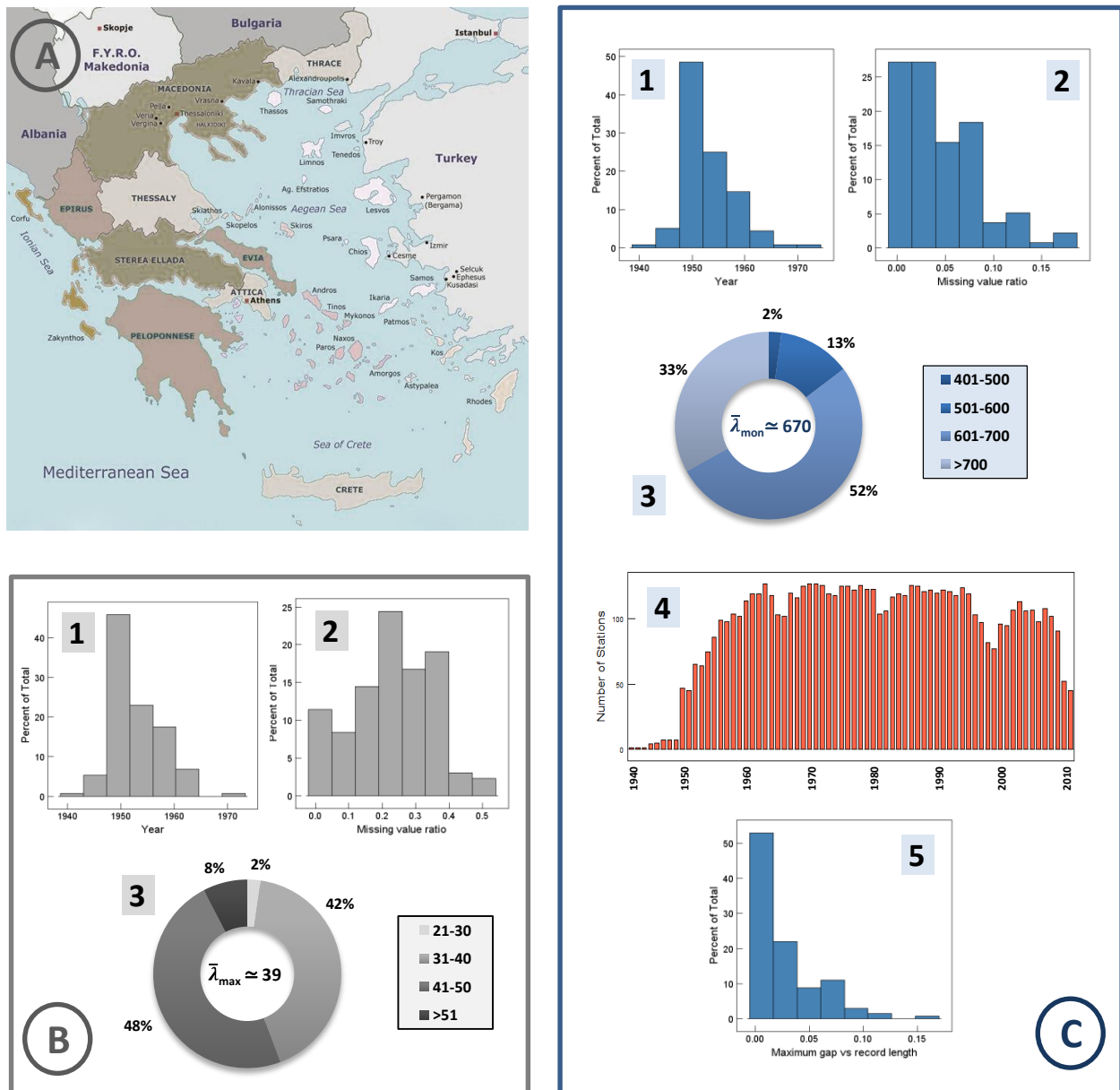


**Figure 1.** A. Geographical setting of the study area; B. Annual daily maxima: 1. Distribution of record start (year), 2. Ratio of missing values versus record length, 3. Distribution of sample size ( $\bar{\lambda}_{max}$  is the mean record length in years); C. Monthly sums: 1. Distribution of record start (year), 2. Ratio of missing values versus record length, 3. Distribution of sample size ( $\bar{\lambda}_{mon}$  is the mean record length in months), 4. Number of stations with all the 12 monthly values per year, 5. Ratio of maximum number of consecutive months with missing values versus record length.

## 2.2 Methods

Initially we investigated the spatial variability of rainfall according to the principles of exploratory data analysis, using the first three moments of data (mean, standard deviation and skewness) and the coefficient of variation (the ratio of the standard deviation versus the mean).

To determine regions with similar precipitation behaviour we used the climate networks approach (Tsonis and Roebber 2004), which utilizes the Pearson correlation coefficient  $\rho_{XY}$  and therefore it can be used to determine regions that present similar temporal fluctuations based on their correlation matrix. To this end each station can be regarded as a network node; when  $\rho_{XY}$  for two stations is above a given threshold, here 0.5, then these stations are considered as *linked*. It should be noted that for the estimation of the correlation coefficient the difference from the average of each monthly mean was used due to the strong seasonality of the annual cycle.

This novel methodological approach allows identifying links between time series with different statistical properties, which however change with a similar manner in time, e.g. two neighbor stations with a large elevation difference. Therefore, its results retain a larger fraction of information regarding the temporal evolution of than other traditional techniques for discrimination, such as principal component analysis or cluster analysis. However, we compared our results with the outcome of two other discrimination methods; *k*-means clustering for mean, standard deviation, coefficient of variation and skewness and hierarchical clustering for correlation, which all presented a similar picture.

The next step involved the aggregation of time series both in time (sum) and space (mean). Spatial aggregation was necessary in order to avoid bias due to the change of station resolution between regions; western Greece for example has a larger number of stations compared to southern Greece. Monthly values were initially summed to hydrological years (October till September) and then spatially to regions with similar properties. If there were any missing monthly values during a year this year was excluded, whereas at least five stations with complete hydrological years should be found per region to estimate their mean values in space for any given year. Slopes were estimated by least squares regression both for each individual station and for the aggregated regions.

A common method to determine slope significance is the non-parametric Mann-Kendal test, used widely in similar studies (Lettenmaier et al. 1994, Serrano et al. 1999, Brunetti et al. 2000, Burn and Hag Elnur 2002, Gemmer et al. 2004, Cannarozzo et al. 2006, Partal and Kahya 2006, Feidas et al. 2007, Rodrigo and Trigo 2007, Xu et al. 2008, Nastos 2011, Zhai et al. 2014). However, this approach assumes independency in time and it has been shown that if this does not hold true the results can be quite misleading (Kulkarni and von Storch 1995, Hamed and Ramachandra Rao 1998, Cohn and Lins 2005). This was also recently acknowledged in the last IPCC report the last IPCC report (Bindoff et al. 2013), suggesting that “*Trends that appear significant when tested against an AR(1) model may not be significant when tested against a process which supports this ‘long-range dependence’.*”

An *autoregressive* process (AR), is a stochastic process whose current value is expressed as a finite, linear sum of the previous values of the process and a white noise term ( $w_i$ ). In discrete time, it can be expressed as:

$$\alpha_i = \lambda_1 \alpha_{i-1} + \lambda_2 \alpha_{i-2} + \dots + \lambda_p \alpha_{i-p} + \underline{w}_i$$

and called an autoregressive process of order  $p$  or AR( $p$ ). The autocorrelation function of the 1<sup>st</sup> order AR process will be  $\rho_i = \lambda^i$ , for  $i \geq 0$ , and it will decay exponentially to zero if  $\lambda > 0$  or will decay exponentially and oscillate in sign if  $\lambda < 0$ . An AR(1) process, is also called a Markov process, because its formulation implies that its future state is only dependent to its present state and not the past ones. Although this simplicity and parsimony made its application very popular, it has been shown that is an ideal case without a plausible physical explanation, not yet verified in the natural phenomena.

Long-range dependence is another term used for Hurst-Kolmogorov (HK) behaviour or long-term persistence. This type of behaviour has been found in many other climatic variables which manifest multi-scale fluctuations (Stephenson et al. 2000, Koutsoyiannis 2003, Markonis and Koutsoyiannis 2013, Tsekouras and Koutsoyiannis 2014). It can be defined by a simple power-law relationship of its standard deviation:

$$\sigma^{(k)} = k^{H-1}\sigma$$

where  $\sigma \equiv \sigma^{(1)}$  and  $H$  is the entropy production in logarithmic time (Koutsoyiannis 2011), more commonly known as the Hurst coefficient and takes on values between 0 and 1. For  $H > 0.5$ , the process exhibits long-term persistence, while for  $H < 0.5$  the process is anti-persistent. Thus, this equation represents a natural behaviour, defines a stochastic process exhibiting this behaviour (the HK process), and describes the stochastic dynamics of this process (the HK dynamics framework). Two noteworthy properties of HK behaviour is the tendency of extremes to cluster in time and the emergence of intense slopes.

Hence, we used a Monte Carlo simulation procedure under three different hypotheses: independency, short-term persistence and long-term persistence. The first hypothesis uses white noise and corresponds to the Mann-Kendal test and is used for comparison reasons with the earlier studies (Xoplaki et al. 2000, Feidas et al. 2007). In the second case (Markov model) the annual rainfall of each year is correlated to the annual rainfall of the previous one as found in longer rainfall records (Kantelhardt et al. 2006, Bunde et al. 2012). And the third case the HK process is used, implying enhanced variability. The procedure followed was rather straightforward. For each hypothesis, a stochastic process was used to create 10 000 synthetic time series of annual rainfall with size equivalent to each regional time series. The processes used were the white noise process, the auto-regressive lag-1, AR(1) process and the Hurst-Kolmogorov process; the latter were produced by the aggregated AR algorithm proposed by Koutsoyiannis (2002). Normality was assumed due to the small record length, which in conjunction with the spatial aggregation procedure mitigated the skewness of the empirical distributions. The slope of each time series was estimated by linear regression and a marginal distribution was determined for each process in order to determine the probability of exceedance for the empirical slopes. Each of the synthetic time series retained the two first moments of the empirical data, in the case of the AR(1) model the correlation coefficient was derived from the original data, whereas for the Hurst-Kolmogorov process the mediocre value of  $H = 0.75$  was given to the Hurst coefficient because the small sample size hinders the estimation of its true value (Koutsoyiannis and Montanari 2007).

All data manipulation, analysis and presentation were done by the R statistical software (R Core Team 2014).

## 4. RESULTS AND DISCUSSION

### *4.1 Variability in space*

The above mentioned strong meridional variability is evident in our findings (Figure 2a). The annual rainfall in the western part of Greece ranges between 900 – 1920 mm, while almost all of the rest annual sums fall between 360 and 720 mm. Standard deviations follow a similar pattern (Figure 2b), but only considering the absolute values; when it comes to the coefficient of variation the pattern changes (Figure 2c) as southern Greece experiences stronger seasonal variability (rainless summers). The majority of the records have a coefficient of variation close to 1.0 (Table 1), while in the south this moves closer to 1.3. A different regime emerges also for skewness (Figure 2d); the north-eastern region is more positively skewed, implying that extremes are more intense in relation to the observed variability. Interestingly, the very same Köppen climate type (Csa) is used to classify the majority of western, central and southern Greece (Malliaros 2013), while their statistical properties differ considerably.

The spatial variability is even more evident if we examine the difference between the minimum and the maximum in the maxima (Table 1; Column 2). The 1147.4 mm observed at Steni station (332m; central Greece) in the December of 2001 is one order of magnitude higher to the maximum monthly rainfall recorded at the station Limnochori (188 mm) which is located at the northern Greece and to a higher altitude (598 m). Most of the stations with the highest monthly maxima lie on the western Greece, while the lowest are found in the continental northern Greece. The most significant deviation from this concerns the Evia stations, three stations in southern-central Greece (with above mentioned Steni station among them) which have elevated means.

**Table 1.** Statistical properties of monthly rainfall per station (columns). Size refers to absolute number of records without any missing values. *Elev* is an abbreviation for elevation, *S.d.* for standard deviation, *C.v.* for coefficient of variation and *Sk.* for skewness.

	Elev. (m)	Max (mm)	Size	Mean (mm)	Median (mm)	S.d. (mm)	C.v.	Sk.
Min	2	188.0	419	28.9	10.7	29.6	0.7	1.0
Max	1000	1147.4	767	158.8	111.4	147.2	1.3	4.7
Mean	340	438.3	668	70.8	51.1	69.0	1.0	1.6
Median	226	403.1	685	60.6	45.6	60.4	1.0	1.5
S.d.	311	188.3	60	29.0	21.5	28.2	0.1	0.4

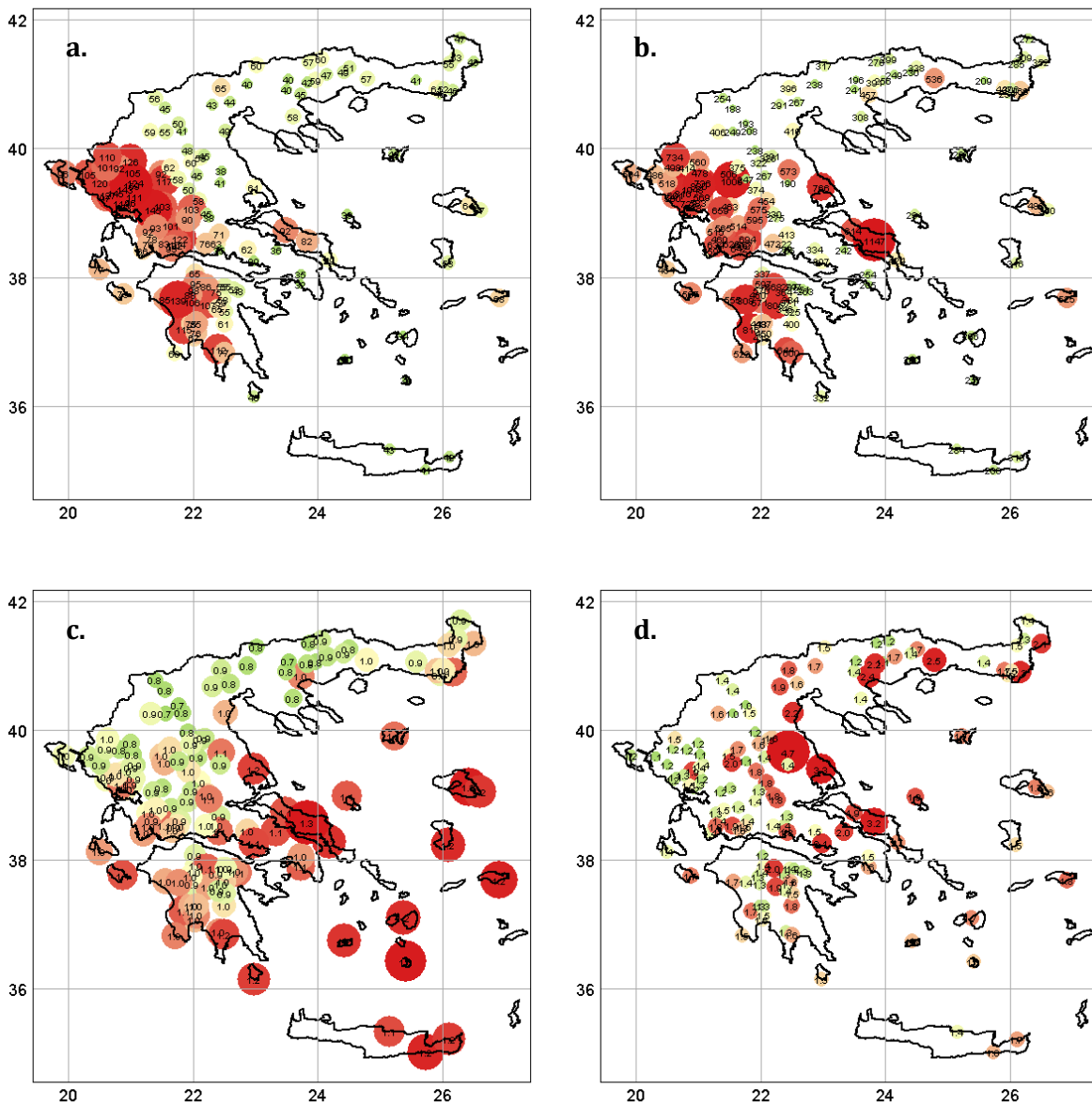


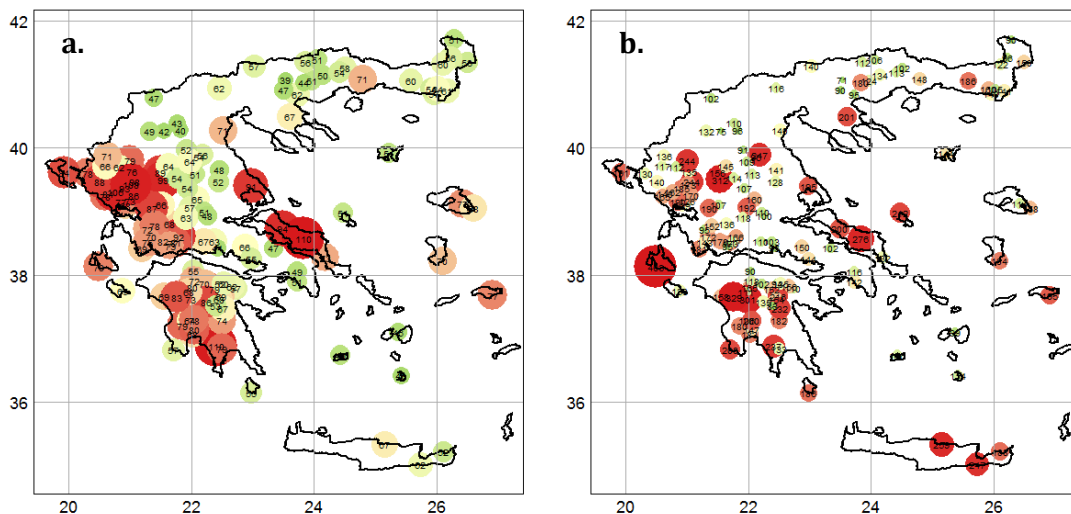
**Figure 2.** Spatial distribution of monthly rainfall: **a.** Mean, **b.** Standard deviation, **c.** Coefficient of variation, **d.** Skewness. Red is used for high values, whereas green for low.

The expected value of the daily maximum per year is close to 100 mm for western Greece and to 50 mm for the rest of the stations, while the absolute maxima range from 71 to 463 mm (Table 2). This picture generally agrees with the monthly rainfall on terms of means and standard deviations (Figures 3a and b), but when it comes to absolute maxima the pattern weakens. Similarly, the coefficient of variance and skewness do not show any distinct pattern, except a below-average set of values in north-western Greece (Figures 3c and d). Interestingly, the coefficient of variation of maxima is not correlated to the skewness, which indicates that there are some locations where there is strong variability in the interannual maximum daily rainfall (high standard deviation, low skewness), and some others that experience single episodes with values quite higher than the expected value (high skewness, low standard deviation).

This means that although each year the expected maxima are higher in western Greece, specific extreme rainfall events can be as high or even higher in the rest of the stations. A possible reason behind this phenomenon could be that the extreme rainfall events might be linked with convective storms and not with the frontal movements. Another possible explanation is that when we investigate extreme events the sample size may not be sufficient to identify possible correlations in space; for example if such events correspond to a return period above 100 years, then 60 years of data of spatially correlated stations would not be enough to determine any spatial relations. In both cases more research is needed to clarify this, which goes beyond the scope of this study.

**Table 2.** Same as Table 1 but for annual maxima of daily rainfall.

	Min (mm)	Max (mm)	Size	Mean (mm)	Median (mm)	S.d. (mm)	C.v.
Min	20.0	71.0	22.0	39.3	36.2	12.0	0.2
Max	76.5	463.0	51.0	109.8	104.0	63.4	0.8
Mean	30.8	151.6	39.1	66.4	62.1	25.1	0.4
Median	28.0	140.2	39.0	65.8	61.0	23.3	0.4
StDev	10.6	56.6	5.4	15.4	15.3	8.0	0.1



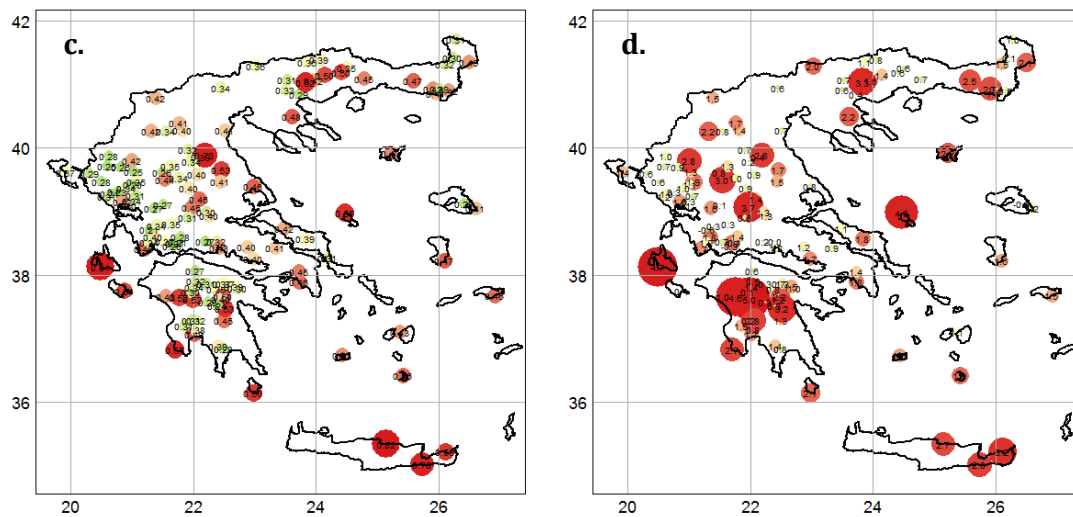


**Figure 3.** Spatial distribution of annual daily maxima: **a.** Mean, **b.** Standard deviation, **c.** Coefficient of variation, **d.** Skewness. Red is used for high values, whereas green for low.

The examination of the correlation matrix between the stations combined with the above findings allowed us to divide the data to eight sets with similar climatic properties (Figure 4; Tables 3 and 4). The application of other discrimination techniques, such as *k*-means clustering to the coefficient of variance (Figure 4d) and hierarchical clustering to the correlation matrix (Figure 4e), confirms our suggested division into sub-regions. In addition, standard deviation or coefficient of variation in space can be considered as simple criteria to compare the uniformity between the groups. Group A (Sterea Hellas) shows the poorest performance; this could be linked to the combined effect of the the relatively small number of stations and the Evia stations, which although they are highly correlated to the rest of the stations, they have quite higher annual sum.

We observe that Western Peloponnesus (P2) has very similar properties with the Western Greece group (W) and therefore it could be argued that they should be merged into a single sub-region. However, more careful examination of Figure 4b shows that P2 is linked to A (Sterea Hellas), whereas W does not. Therefore, if the two sub-regions are fused into a single then this could mask some information about the the spatial diversity of temporal variability. Another example can be found between regions A and C (Central Greece), which are even more identical in terms of statistical properties. Again in Figure 4b, we can see that this neighboring regions are not linked, which means that they demonstrate different behavior in time. These two examples, show some of the potential benefits of the Climate Networks method, which could be missed by traditional clustering techniques. In addition, the spatial dependence structure of the examined area can be studied in detail; e.g. the long-range correlation between rainfall in western and eastern Greece and the stronger correlations between stations within regions W, P1 and P2 compared to the other regions.

In order to further validate our results we compared the aggregated time-series with high-resolution gridded data, provided by Koninklijk Nederlands Meteorologisch Instituut, KNMI, (E-OBS 0.25° dataset). There was good correspondence between and some long-range correlations with central and western Mediterranean were found for the western regions (Figure 5a-c). This is also confirmed by other researchers and linked with general circulation patterns (Dünkeloh and

Jacobeit 2003). Interestingly, it seems that different regions of Greece, e.g. region A (Figure 5d-f), is not correlated in the same manner in larger spatial scales.

Daily maxima properties present a similar behaviour to the annual regime when it comes to their means and standard deviations. However, the mean of the absolute maxima is very close for all areas ranging from 140 to 170 for all the groups but northern Greece (N). The southern areas (A, P1, S) experience the highest values followed by the western (W, P2), while the northern the lowest. This strengthens our hypothesis that extreme rainfall events might not be linked with neither large scale atmospheric circulation or topography and also suggest a possible link to the meridonal temperature gradient. The southern records (A, P1, P2 and S) also show higher skewness, due to the existence of some very high maxima among them.

Annual rainfall is also connected to the topography in terms of elevation (Gouvas et al. 2009). As we aggregate the time-series in space this could introduce bias in the regional time series if the majority of the stations in a group are in higher altitude than the others. To verify that the threshold of 1000 m is sufficient for station elevation we compared the correlation between annual rainfall and longitude and annual rainfall and elevation (Figure 6). It is evident that the link to the latitude is stronger and can be regarded as a better descriptor of the expected annual rain than station altitude (when it is less than 1000 m).

**Table 3.** Statistical properties of annual rainfall (hydrological years) per group of stations. *S.d.s* and *S.d.v.* are the standard deviation in space and time correspondingly, *C.v.s* and *C.v.t* are the coefficients of variation in space and time respectively and *ACF* is the auto-correlation function coefficient for lag equal to 1 year. Highest values are highlighted with **bold**, while minima are presented with *italics*.

Id	Area	# of stations	Elev. (m)	Mean (mm)	S.d.s. (mm)	S.d.t (mm)	C.v.s.	C.v.t.	Sk.	ACF (lag 1)
E	East	14	<i>53</i>	624	99	200	0.16	<b>0.32</b>	0.45	0.23
N	Northern Greece	24	353	605	94	166	0.16	0.27	<i>0.15</i>	<b>0.30</b>
C	Central Greece	21	405	722	259	200	0.36	0.28	0.24	0.20
A	South, Sterea Hellas	9	129	633	<b>267</b>	181	<b>0.42</b>	0.29	<b>0.50</b>	<b>0.33</b>
P1	Eastern Peloponnesus	10	<b>638</b>	700	90	168	<i>0.13</i>	<i>0.24</i>	<i>0.15</i>	<i>-0.02</i>
P2	Western Peloponnesus	19	436	1047	264	274	0.25	0.26	0.25	0.14
W	West	<b>33</b>	374	<b>1266</b>	262	<b>305</b>	0.21	<i>0.24</i>	<b>0.54</b>	0.10
S	South, Islands	<i>6</i>	60	<i>452</i>	<i>65</i>	<i>117</i>	0.14	0.27	0.39	0.04

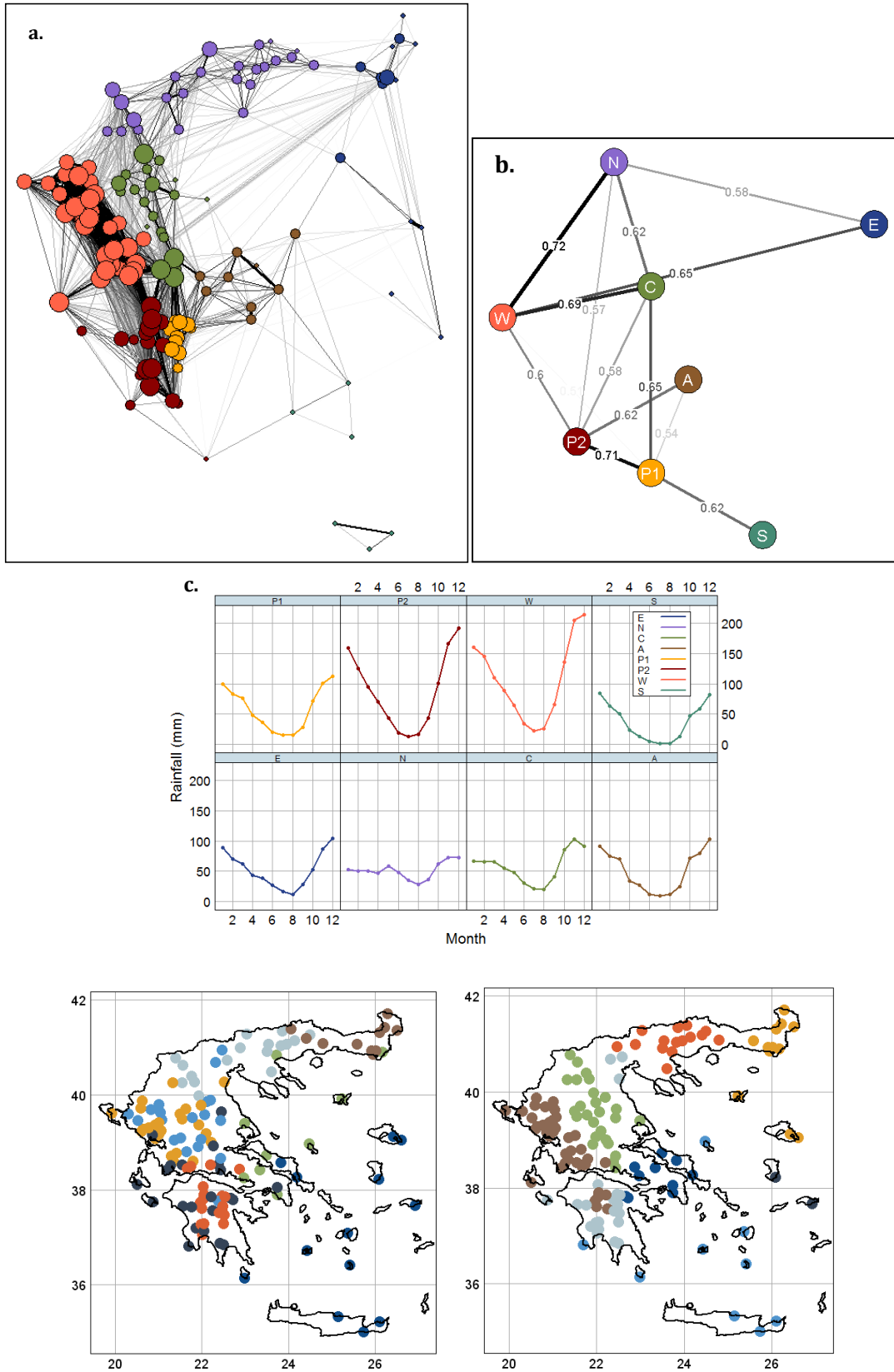


**Figure 4.** **a.** Correlation network of the monthly differences; size of circles corresponds to the number of links with other stations. **b.** Correlation network of the aggregated time series in the annual time scale. **c.** Monthly distribution of rainfall per group. **d.** *k*-means clustering. **e.** Hierarchical clustering.

**Table 4.** As Table 3 but for annual daily maxima. *Max* is absolute maximum observed in each group of stations, while *m. Max* is the mean of all absolute maxima per group.

Id	Area	Mean (mm)	S.d.s. (mm)	S.d.t. (mm)	Max (mm)	m. Max (mm)	$\mu$ to <i>M</i>	<i>A</i> to $\mu$	Sk.
E	East	61	9	24	195	142	2.3	1.2	1.34
N	Northern Greece	53	10	22	201	119	2.3	1.0	1.23
C	Central Greece	61	15	24	313	141	2.3	1.1	1.24
A	South, Sterea Hellas	66	22	27	276	164	2.5	1.3	1.57
P1	South, Eastern Peloponnesus	64	9	25	328	170	2.3	1.1	1.35
P2	South, Western Peloponnesus	73	13	28	232	152	2.3	0.8	1.44
W	West	78	11	25	463	163	2.1	0.8	1.06
S	South, Islands	53	9	31	259	170	3.1	1.4	2.21

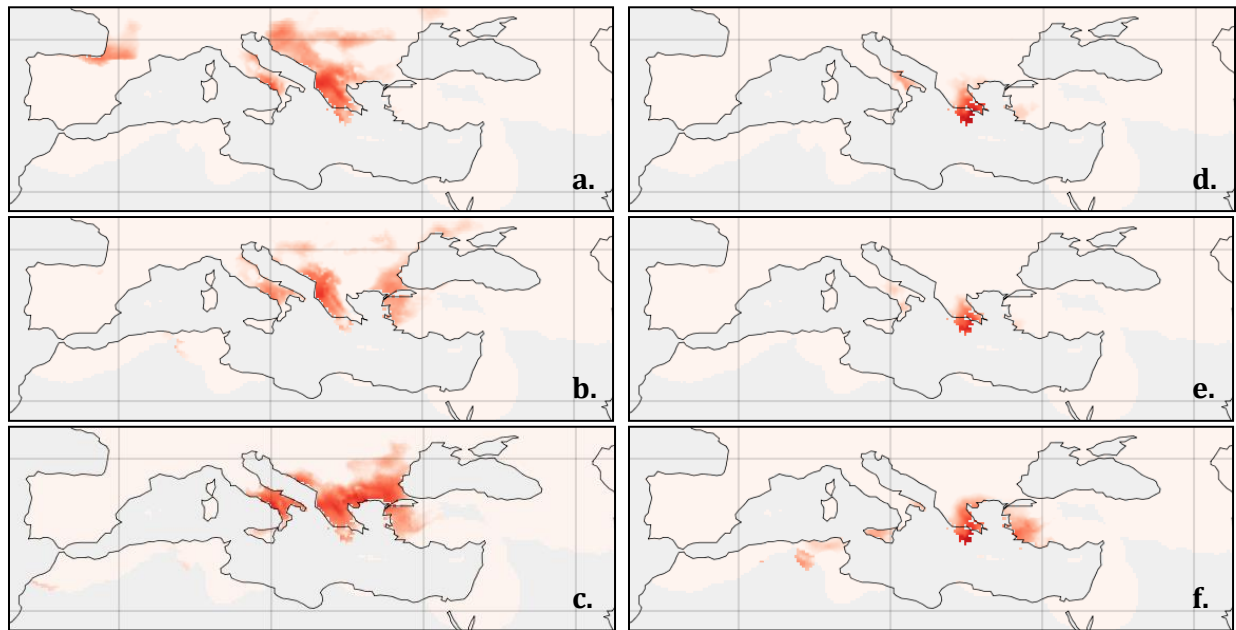


**Figure 5.** Correlation of annual rainfall of group W (a. – c.) and A (d. – f.) with winter rainfall in the Mediterranean region (December to February). Each point above 0.5 is depicted as gradient of red colour.

Furthermore, if we apply simple linear regression to make a crude estimate of how rainfall changes with elevation some remarks may be made (Table 5). Group C has the best fit and the overall estimate for the rainfall increase due to elevation could range between 30 – 60 mm per 100 m for continental Greece (however the uncertainty is high). The low slope of group N is possibly linked with the prevailing low winter temperatures of northern Greece and snowfall; while the high slope at group A could be an artifact due to the group heterogeneity (also discussed above). All the stations in groups E and S are below 200 m and thus  $R^2$  values are close to zero and no conclusion can be made for these stations. A final remark could be that below 1000 m in the western regions of Greece the mean annual rain is higher even though the mean elevation of the stations is lower, which is indicative of the difference between the western and eastern precipitation regimes.

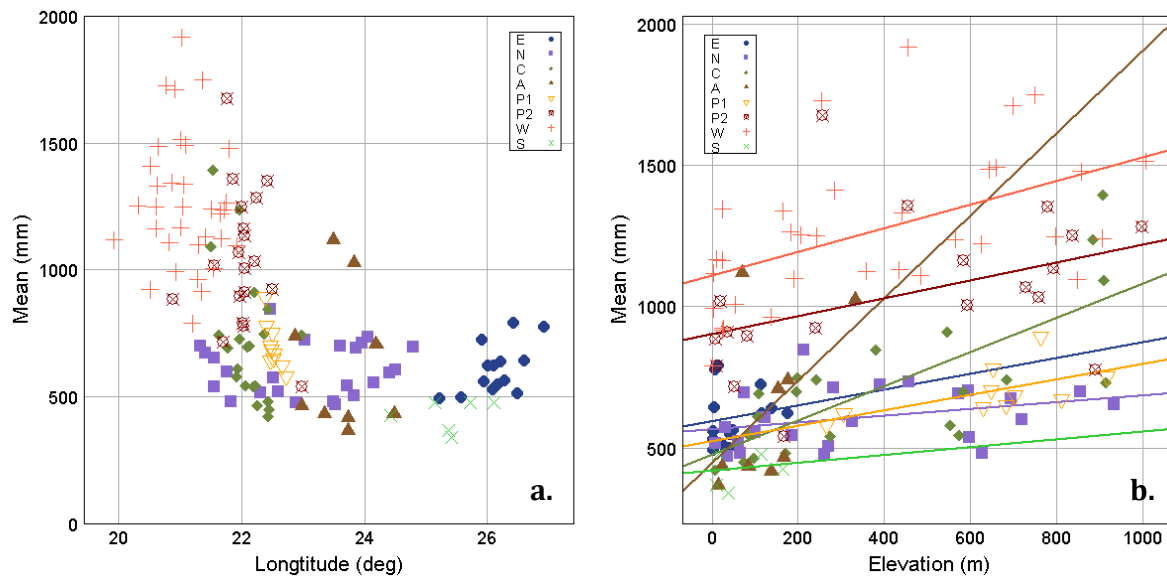


**Figure 6.** Correlation between mean annual rainfall and **a.** longitude, **b.** elevation.

**Table 5.** Results of linear regression per group of stations.

Group	Slope	Intercept	$R^2$
E	0.28	594	0.03
N	0.12	566	0.11
C	0.60	477	0.55
A	1.46	446	0.25
P1	0.27	526	0.38
P2	0.32	904	0.18
W	0.42	1110	0.26
S	0.14	420	0.02

#### 4.2 Variability in time

Rainfall over Greece exhibits strong variability in time in both annual and decadal scale (Figure 7). Aggregation of the group time series in the annual scale (hydrological year) showed that rainfall does not vary in the same way at each region. However, at larger scales such as the decadal, it can be seen that during the decade 1956-66 was the wettest for most of the regions, while the driest period can be found during the years between 1985 and 1995. In the first period the annual rainfall reached its maximum in most of the stations in the hydrological year 1963-1964, while during the dry decade the majority of minima can be found during 1990-91. Notably, maxima and minima at the mean of the daily maxima did not occur during these periods; 1950-51 was the year with the highest mean of daily maxima and 1974-75 the year with the lowest.

The examination of the slopes of the annual rainfall for each station showed an overall decrease all over Greece (Figure 8). The slopes are sharper at western Greece and almost inexistent at central and southern Greece and the region close to Athens. These findings are in a good agreement with prior research results (Xoplaki et al. 2000, Maheras and Anagnostopoulou 2003, Maheras et al. 2004, Feidas et al. 2007, Kambezidis et al. 2010, Philandras et al. 2011), as the western part of

Greece is linked more closely to the atmospheric circulation over the Mediterranean Sea and NAO in specific, and hence it could be linked with its persistent positive phases during 1980-2000 (Xoplaki et al. 2000, Maheras and Anagnostopoulou 2003, Feidas et al. 2007). This is also reflected in the aggregated groups of stations: five of them presented a decline in annual rain, two remained steady, and only one showed an increase (Table 6). Furthermore, the groups that do not show any decrease (P1, S and A) are the groups with the smallest number of stations, which increases the uncertainty of these findings.

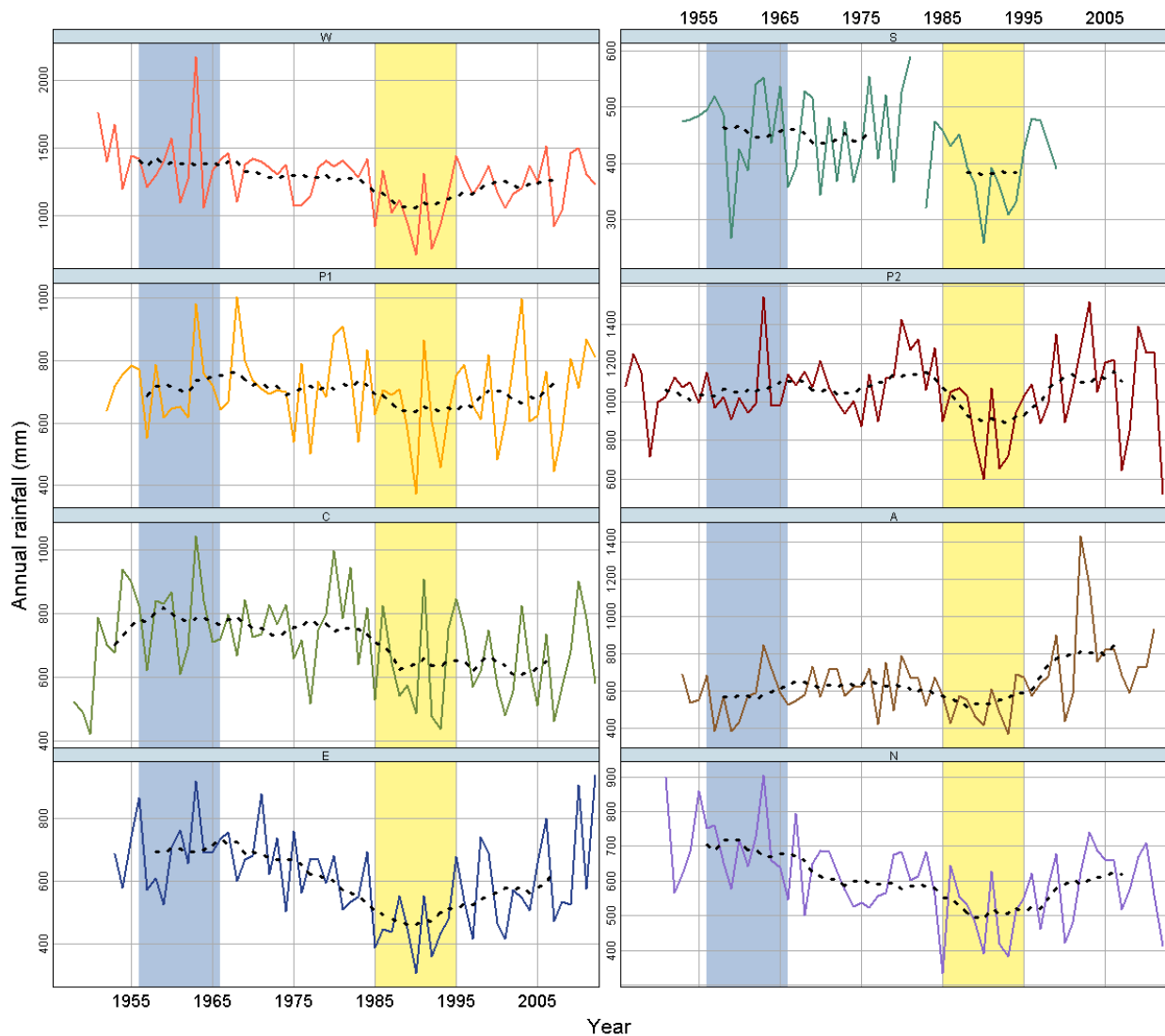


**Figure 7.** Aggregated time series (hydrological years) per group of stations and their decadal moving average (dashed lines). Light blue and yellow blocks depict the wettest and driest decades based on the decadal mean of all stations.



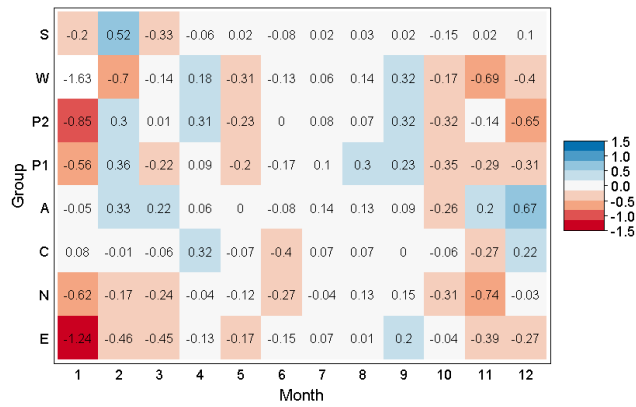


**Figure 9.** Monthly rainfall slopes per region.

As discussed in the Methods section, the estimation of the statistical significance of the slopes is a crucial step in the discrimination between inherent natural variability and causal links with specific physical processes. A widely used statistical tool in climatology to assess slope significance is the non-parametric Mann-Kendal test, which assumes independency in time as in the case of a ‘white noise’ model (WN). However, this assumption rarely holds true in geophysical time series and therefore it would be erroneous to use the Mann-Kendal test without estimating the auto-correlation structure of the variable. In our case, the lag 1 auto-correlation coefficient ranges between 0 and 0.3, i.e. white noise and weak dependence.

However, independency cannot be assumed so easily, even if the auto-correlation coefficient is close to zero due to the relatively small sample size. Studies in datasets with sample sizes close to 100 values argue that annual rainfall demonstrates short term persistence and should be modeled by an auto-regressive and not an HK process (Kantelhardt et al. 2006, Bunde et al. 2012). On the other hand, it has been shown that even though precipitation records may exhibit no or short-term correlation in smaller scales, when scales grow HK behaviour emerges (Fraedrich and Larnder 1993, Pelletier and Turcotte 1997). Another indication supportive to the use of the HK model in rainfall records comes by the investigation of paleoclimatic data; different precipitation reconstructions were found to exhibit strong HK behaviour (Bunde et al. 2013, Markonis and Koutsoyiannis 2016, Iliopoulou et al. in press). In our study area the estimation of the  $H$  coefficient for annual rainfall with the LSV-H method (Koutsoyiannis 2002, Tyralis and Koutsoyiannis 2011) showed that most stations have values in the 0.7 to 0.8 interval (Figure 10). Therefore all three hypotheses should be taken into account.

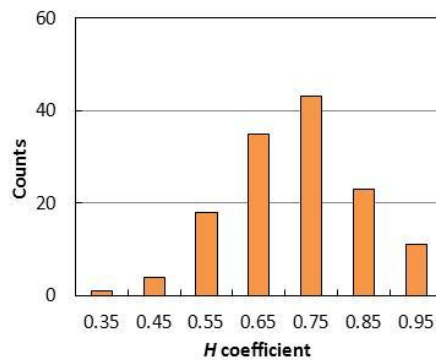


**Figure 10.** Distribution of  $H$  values for annual rainfall per station

The results can be found at Table 6. We can see that the region with the highest absolute decrease is W, while in it comes to the relation to the annual mean groups E and N prevail. Is this change statistically significant though? Monte Carlo simulation clearly shows that the answer is highly dependent on the statistical framework used. Thus, depending on the assumption made, the maximum observed change occurs at Northern Greece (N) and could be described as extremely rare (independency hypothesis;  $\min(p)=0.0006$ ), rare (short-term persistence hypothesis;  $\min(p)=0.09$ ) or uncommon (HK dynamics hypothesis;  $\min(p)=4.2$ ). For all three hypotheses P1 and P2 are the regions which do not present any significant change. The results for winter rainfall are similar, with Eastern Greece (E) slopes becoming the most significant and C and A, sharing the same non-significant behaviour of P1 and P2.

Furthermore, uncertainty is influenced by the homogeneity of each group and its total number of stations, which increases our reluctance for the results about the group A; two of the stations are located in the capital, where they might be affected by the thermal island phenomenon and two in the Evia island (see section 4.1) in a total of 9 stations. The low number of stations should also be taken into consideration for the findings of region S. The same steps were followed for mean daily maxima per year, but no significant slope was identified except for groups A and C, even for the WN assumption. Notably, the linear correlation between mean daily maxima and annual sums (second column in Table 6) does not keep up with change in longer terms, which is also confirmed by previous studies (Kostopoulou and Jones 2005, Kambezidis et al. 2010).

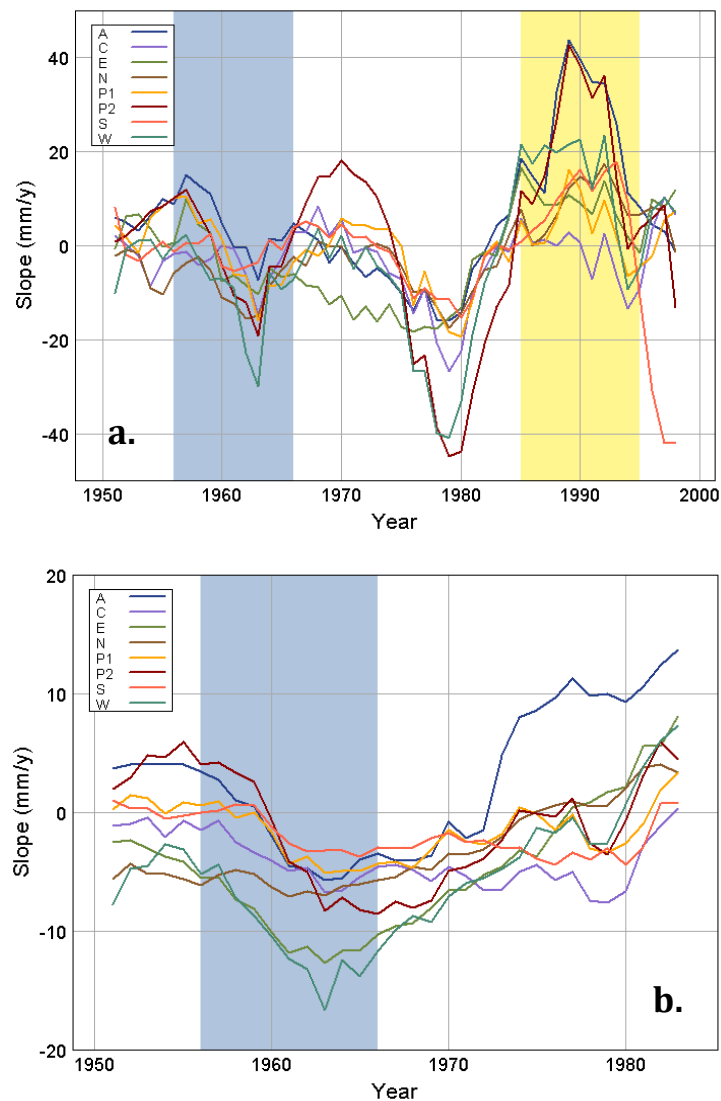
**Table 6.** Slope per region (annual and January rainfall) and the probability of exceedance  $P(x)$  for three different statistical models;  $\rho_1$  is the autocorrelation coefficient for lag 1 year, while  $\rho_{XY}$  is the Pearson correlation coefficient between annual sum and mean daily maximum per year.

Group			Slope $b$		$P(x) >  b  (\times 10^{-2})$			Same for January		
	$\rho_1$	$\rho_{XY}$	(mm/y)	(%)	WN	AR(1)	HK	WN	AR(1)	HK
E	0.23	0.60	-2.61	-0.42	0.7	2.6	10.0	0.04	1.1	4.3
N	0.30	<b>0.65</b>	-2.71	-0.44	0.06	1.1	4.2	0.4	1.1	7.8
C	0.20	0.50	-2.75	-0.35	3.7	7.7	17.2	38.3	39.7	44.4
A	<b>0.34</b>	0.59	<b>3.69</b>	<b>0.58</b>	0.3	3.2	6.7	44.3	44.6	46.3
P1	-0.01	0.41	-0.55	-0.08	28.6	27.7	38.2	7.2	8.0	22.4
P2	0.14	0.32	-0.29	-0.03	41.8	42.4	45.9	3.9	9.6	18.6
W	0.10	0.55	-4.32	-0.33	0.5	0.9	8.5	0.4	4.8	8.6
S	0.04	0.29	-1.11	-0.26	11.8	11.9	24.7	34.2	32.9	40.2

There is also a final observation that advocates of the plausibility of the HK dynamics. Examination of the slopes under different temporal scales and time windows (moving slopes) showed that they are not constant in time but they constantly change value and sign (Figures 11a and b). For example, we can see that during the last 15 years rainfall over Greece has remained rather stable, but during the last 30 years there was a discernable increase, while since the 1950s rainfall has declined. This kind of change could be the result of simultaneous processes in different scales, which is another property of HK dynamics (Koutsoyiannis 2002). Notably, if the Monte Carlo method is used to establish the 5% confidence intervals for the change in slope of each model (white noise, AR(1) and HK), then the HK process is the one that encloses the majority of the observed slopes. The increase of the last 30-years (Figures 11a) may imply a raise in the cyclonic activity (Maheras et al. 2004, Tolika et al. 2007) or/and enhanced southern meridional flow (Feidas

et al. 2007 and references within). Possible explanations can also be linked with general atmospheric circulation, i.e. changes in NAO behaviour or the other indices linked with rainfall over Eastern Mediterranean.

The moving slope approach shows that in smaller scales (Figure 11a) each region behaves differently, while in larger scales (Figure 11b) there is a convergence. This can be seen more easily, if a constant point in time is taken, such as the first (Figure 11c) or the last (Figure 11d) points of our records are taken and calculate each slope starting at a 15 year-window, which is stretched to the full record. Convergence emerges at 40-50 years, which is the point that the standard deviation of each record becomes relatively stable. However, even in these time windows the slope of some regions may differ; for example in Figures 11c and d, the northern regions (W, N, E, C) finally converge between -2.5 to -5 mm/y, while the southern (P1, P2, S) are close to zero (again region A shows quite different behaviour). On the other hand, it seems that the periods with maximum or minimum rainfall (decades 1956-1966 and 1985-1995 correspondingly) are encountered almost synchronously, which could imply that the rainfall extremes in space are linked to the extremes in time.



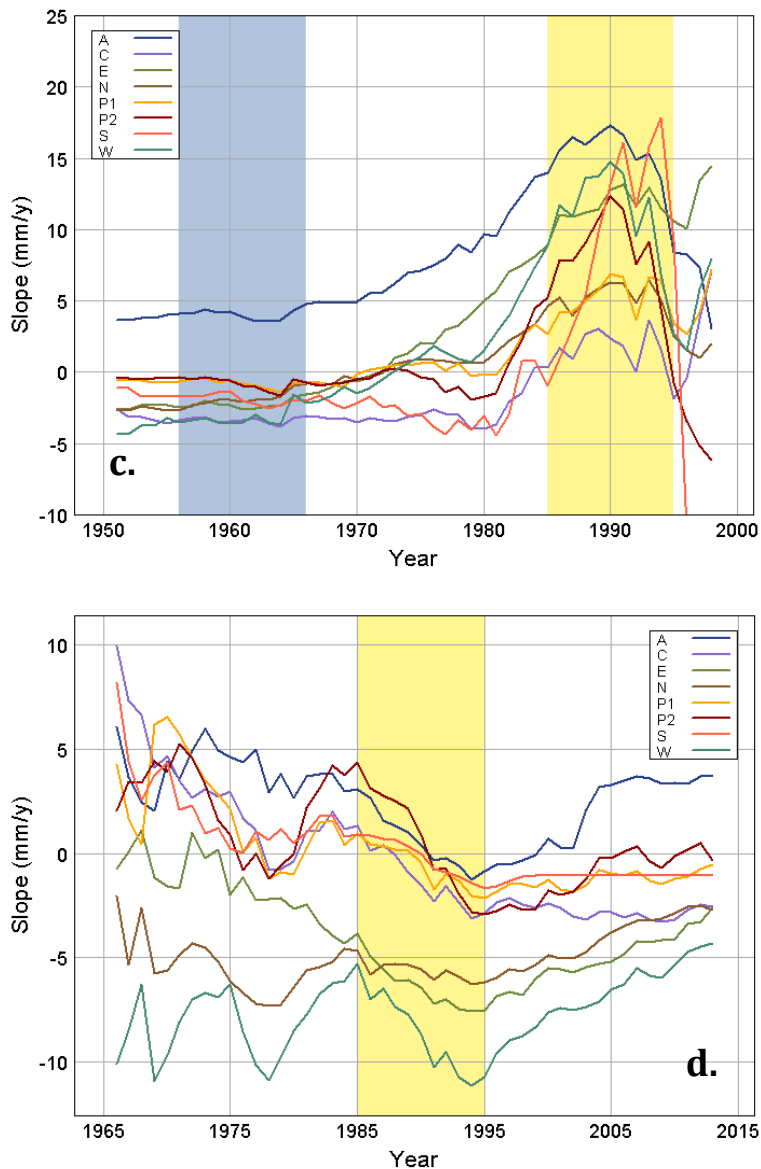


**Figure 11.** The slope of rainfall per region in different time windows: **a.** 15 years, **b.** 30 years, **c.** starting at 1997 and extending backwards (and the corresponding standard deviation **e.**), **d.** starting at 1951 and extending forwards

Finally, we compared our findings with Coupled Model Intercomparison Project Phase 5 (CMIP5) ensemble mean derived from KNMI database (Figures 12a and b). For this purpose we have chosen the region *W* because, as discussed above, it has the largest number of stations, it features strong homogeneity and it is correlated to the Mediterranean regional climates and to the general atmospheric circulation. One can see that there is a strong discrepancy, especially as we move to the 30-year scale. Such discrepancies have already been highlighted (Koutsoyiannis et al. 2008, Anagnostopoulos et al. 2010) and are also confirmed in our case, suggesting that GCMs still present some strong deficiencies in describing regional climate variability even in larger scales.

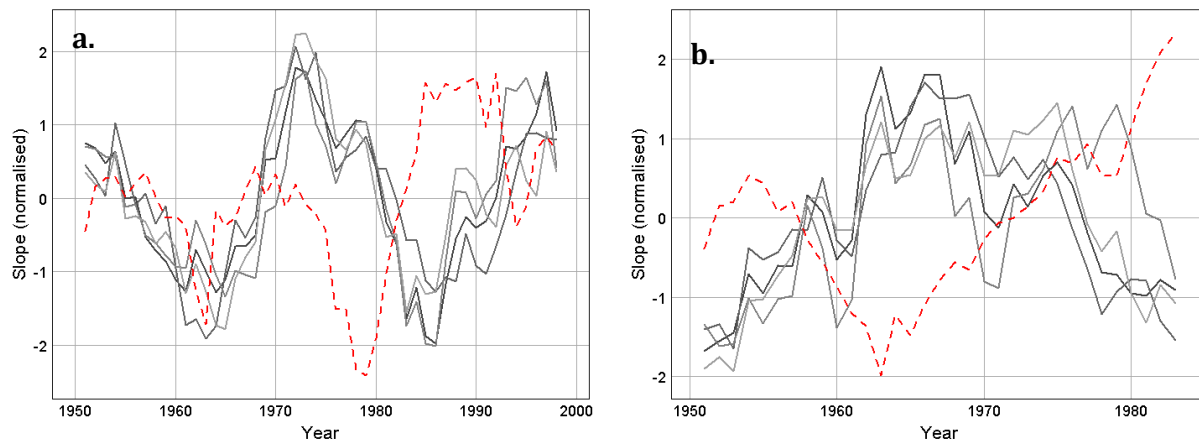


**Figure 12.** Comparison of moving slopes for **a.** 15-year and **b.** 30-year time windows between region W (dashed red line) and different CMIP5 scenario ensemble means (rcp26, rcp45, rcp60, rcp85; grey solid lines). The slopes were normalized since CMIP data were in  $\text{kg m}^{-2} \text{s}^{-1}$ .

## 5. CONCLUSIONS

Our study suggests that decadal variability of precipitation over Greece is quite strong and emerges in different temporal and spatial scales. Most regions show a decline since 1950, an increase since 1980 and remain stable during the last 15 years; however these changes are not uniform in space. Such multi-scale fluctuations are indicative of Hurst-Kolmogorov behaviour, which was confirmed (mean  $H = 0.75$ ). Interestingly, this value is significantly higher by the global average ( $H = 0.6$ ) as estimated by Iliopoulou et al. (in press) and might be linked with the complexity of the processes that affect the Mediterranean climate.

A direct impact of HK behaviour can be found in the overestimation of slope significance (Cohn and Lins, 2005). This is also the case for the Greek territory, where previous studies (Xoplaki et al. 2000, Feidas et al. 2007) based solely on Mann-Kendal test resulted to statistically significant reduction of winter and annual precipitation. Here, we showed that if the HK assumption holds true the observed change in precipitation is not so rare and can be attributed to natural variability. Therefore strong shifts in decadal mean will be encountered more often than the previous studies imply; a result with a noteworthy impact to water resource management.

In the same context, our findings of increased variability offer a probable explanation of the antithesis between the observed change in precipitation over Greece and the latest results of the CMIP5 experiment. Such discrepancies have also been confirmed for the entire Mediterranean region, as “*observational precipitation and evaporation records also include decadal variations that are larger than the above-mentioned simulated long-term trends (e.g. for precipitation, observed decadal anomalies are about two orders of magnitude larger than the simulated trend)*” (Mariotti, 2011). Again, significant implications in the successful design and management of future hydraulic works can be found here, because it is a common practice to use the GCM multi-decadal forecasts as input to regional hydrological models.

Quantifying natural variability in climate is a major challenge of our era, also acknowledged in the last IPCC report (Bindoff et al. 2013). We have showed that the Hurst-Kolmogorov stochastic

framework can be a useful tool to determine the magnitude of natural fluctuations and provided some insight of the enhanced uncertainty of the precipitation variability over Greece.

## ACKNOWLEDGMENTS

Y. Markonis and D. Koutsoyiannis would like to acknowledge that they have been financed by the European Union (European Social Fund – ESF) and Greek national funds through the Operational Program “Education and Lifelong Learning” of the National Strategic Reference Framework (NSRF) – Research Funding Program: ARISTEIA II: Reinforcement of the interdisciplinary and/ or inter-institutional research and innovation (CRESENDO project; grant number 5145).

The authors would like also would like to thank Prof. N. Mamassis for his valuable comments and advise, as well as the anonymous reviewers for their constructive remarks.

## REFERENCES

- Anagnostopoulos, G., D. Koutsoyiannis, A. Christofides, A. Efstratiadis, and N. Mamassis. 2010. A comparison of local and aggregated climate model outputs with observed data. *Hydrological Sciences Journal–Journal des Sciences Hydrologiques* **55**:1094-1110.
- Bindoff, N.L., P.A. Stott, K.M. AchutaRao, M.R. Allen, N. Gillett, D. Gutzler, K. Hansingo, G. Hegerl, Y. Hu, S. Jain, I.I. Mokhov, J. Overland, J. Perlwitz, R. Sebbari and X. Zhang, 2013. Detection and Attribution of Climate Change: from Global to Regional. In: *Climate Change 2013: The Physical Science Basis. Contribution of Working Group I to the Fifth Assessment Report of the Intergovernmental Panel on Climate Change* [Stocker, T.F., D. Qin, G.-K. Plattner, M. Tignor, S.K. Allen, J. Boschung, A. Nauels, Y. Xia, V. Bex and P.M. Midgley (eds.)]. Cambridge University Press, Cambridge, United Kingdom and New York, NY, USA.
- Bolle, H.-J. 2003. Mediterranean climate: variability and trends. Springer.
- Brunetti, M., L. Buffoni, M. Maugeri, and T. Nanni. 2000. Precipitation intensity trends in northern Italy. *International Journal of Climatology* **20**:1017-1031.
- Bunde, A., U. Büntgen, J. Ludescher, J. Luterbacher, and H. von Storch. 2013. Is there memory in precipitation? *Nature Climate Change* **3**:174-175.
- Bunde, A., M. I. Bogachev, and S. Lennartz. 2012. Precipitation and River Flow: Long-Term Memory and Predictability of Extreme Events. *Extreme Events and Natural Hazards: The Complexity Perspective*:139-152.
- Burn, D. H., and M. A. Hag Elnur. 2002. Detection of hydrologic trends and variability. *Journal of Hydrology* **255**:107-122.
- Cannarozzo, M., L. Noto, and F. Viola. 2006. Spatial distribution of rainfall trends in Sicily (1921–2000). *Physics and Chemistry of the Earth, Parts A/B/C* **31**:1201-1211.
- Cohn, T. A., and H. F. Lins. 2005. Nature's style: Naturally trendy. *Geophysical Research Letters* **32**.
- Cullen, H. M., and P. B. Demenocal. 2000. North Atlantic influence on Tigris–Euphrates streamflow. *International Journal of Climatology* **20**:853-863.
- Dünkeloh, A., and J. Jacobeit. 2003. Circulation dynamics of Mediterranean precipitation variability 1948–98. *International Journal of Climatology* **23**:1843-1866.
- Eshel, G., and B. F. Farrell. 2000. Mechanisms of eastern Mediterranean rainfall variability. *Journal of the atmospheric sciences* **57**:3219-3232.
- Feidas, H., C. Nouloupoulou, T. Makrogiannis, and E. Bora-Senta. 2007. Trend analysis of precipitation time series in Greece and their relationship with circulation using surface and satellite data: 1955–2001. *Theoretical and Applied Climatology* **87**:155-177.
- Fraedrich, K., and C. Larnder. 1993. Scaling regimes of composite rainfall time series. *Tellus A* **45**:289-298.
- Gemmer, M., S. Becker, and T. Jiang. 2004. Observed monthly precipitation trends in China 1951–2002. *Theoretical and Applied Climatology* **77**:39-45.
- González-Hidalgo, J., M. De Luis, J. Raventós, and J. Sánchez. 2001. Spatial distribution of seasonal rainfall trends in a western Mediterranean area. *International Journal of Climatology* **21**:843-860.
- Gouvas, M., N. Sakellariou, and F. Xystrakis. 2009. The relationship between altitude of meteorological stations and average monthly and annual precipitation. *Studia Geophysica et Geodaetica* **53**:557-570.

- Griggs, D. J., and M. Noguer. 2002. Climate change 2001: the scientific basis. Contribution of working group I to the third assessment report of the intergovernmental panel on climate change. *Weather* **57**:267-269.
- Hamed, K. H., and A. Ramachandra Rao. 1998. A modified Mann-Kendall trend test for autocorrelated data. *Journal of Hydrology* **204**:182-196.
- Hatzaki, M., Flocas, H. A., Asimakopoulos, D. N., & Maheras, P. 2007. The eastern Mediterranean teleconnection pattern: identification and definition. *International Journal of Climatology*, **27**(6):727-737.
- Hatzaki, M., Flocas, H. A., Giannakopoulos, C., & Maheras, P. 2009. The impact of the eastern Mediterranean teleconnection pattern on the Mediterranean climate. *Journal of Climate*, **22**(4):977-992.
- Houghton, J. T. 1996. *Climate change 1995: The science of climate change: contribution of working group I to the second assessment report of the Intergovernmental Panel on Climate Change*. Cambridge University Press.
- Iliopoulou T., S. M. Papalexiou, Y. Markonis and D. Koutsoyiannis, 2016, Revisiting long-range dependence in annual precipitation, *Journal of Hydrology*, in press.
- Hurrell, J. W. 1995. Decadal trends in the North Atlantic Oscillation: regional temperatures and precipitation. *Science* **269**:676-679.
- Hurst, H. E. 1951. {Long-term storage capacity of reservoirs}. *Trans. Amer. Soc. Civil Eng.* **116**:770-808.
- Kambezidis, H. D., I. K. Larissi, P. T. Nastos, and A. G. Paliatsos. 2010. Spatial variability and trends of the rain intensity over Greece. *Adv. Geosci.* **26**:65-69.
- Kantelhardt, J. W., E. Koscielny-Bunde, D. Rybski, P. Braun, A. Bunde, and S. Havlin. 2006. Long-term persistence and multifractality of precipitation and river runoff records. *Journal of Geophysical Research: Atmospheres* (1984–2012) **111**.
- Kendall, M. G. 1948. Rank correlation methods.
- Kolmogorov, A. N. 1940. Wiener'sche Spiralen und einige andere interessante Kurven im Hilbertschen Raum. Pages 115-118 in *CR (Dokl.) Acad. Sci. URSS*.
- Kostopoulou, E., and P. Jones. 2005. Assessment of climate extremes in the Eastern Mediterranean. *Meteorology and Atmospheric Physics* **89**:69-85.
- Kostopoulou, E., and P. D. Jones. 2007. Comprehensive analysis of the climate variability in the eastern Mediterranean. Part II: relationships between atmospheric circulation patterns and surface climatic elements. *International Journal of Climatology* **27**:1351-1371.
- Koutsoyiannis, D. 2002. The Hurst phenomenon and fractional Gaussian noise made easy. *Hydrological Sciences Journal* **47**:573-595.
- Koutsoyiannis, D. 2003. Climate change, the Hurst phenomenon, and hydrological statistics. *Hydrological Sciences Journal* **48**:3-24.
- Koutsoyiannis, D., A. Efstratiadis, N. Mamassis, and A. Christofides. 2008. On the credibility of climate predictions. *Hydrological Sciences Journal* **53**:671-684.
- Koutsoyiannis, D., and A. Montanari. 2007. Statistical analysis of hydroclimatic time series: Uncertainty and insights. *Water resources research* **43**.
- Koutsoyiannis D. 2011. Hurst–Kolmogorov dynamics as a result of extremal entropy production. *Physica A: Statistical Mechanics and its Applications*, **390**(8): 1424-1432.
- Krichak, S. O., and P. Alpert. 2005. Decadal trends in the east Atlantic–west Russia pattern and Mediterranean precipitation. *International Journal of Climatology* **25**:183-192.
- Kulkarni, A., and H. von Storch. 1995. Monte Carlo experiments on the effect of serial correlation on the Mann-Kendall test of trend. *Meteorologische Zeitschrift* **4**:82-85.
- Kutiel, H., P. Maheras, and S. Guika. 1996. Circulation indices over the Mediterranean and Europe and their relationship with rainfall conditions across the Mediterranean. *Theoretical and Applied Climatology* **54**:125-138.
- Lettenmaier, D. P., E. F. Wood, and J. R. Wallis. 1994. Hydro-climatological trends in the continental United States, 1948-88. *Journal of Climate* **7**:586-607.
- Lionello, P. 2012. *The Climate of the Mediterranean Region: From the Past to the Future*. Elsevier.
- Maheras, P., and C. Anagnostopoulou. 2003. Circulation Types and Their Influence on the Interannual Variability and Precipitation Changes in Greece. Pages 215-239 in H.-J. Bolle, editor. *Mediterranean Climate*. Springer Berlin Heidelberg, Berlin, Heidelberg.
- Maheras, P., K. Tolika, C. Anagnostopoulou, M. Vafiadis, I. Patrikas, and H. Flocas. 2004. On the relationships between circulation types and changes in rainfall variability in Greece. *International Journal of Climatology* **24**:1695-1712.
- Malliaros, A. 2013. Investigation of climate variability accordance with the classification KÖPPEN. Thesis. National Technical University of Athens.

- Mann, H. B. 1945. Nonparametric tests against trend. *Econometrica: Journal of the Econometric Society*:245-259.
- Mariotti A., 2011, Decadal Climate Variability and Change in the Mediterranean Region, US National Oceanic and Atmospheric Administration, Climate Test Bed Joint Seminar Series, NCEP, Maryland, USA.
- Markonis, Y., and D. Koutsoyiannis. 2013. Climatic variability over time scales spanning nine orders of magnitude: Connecting Milankovitch cycles with Hurst–Kolmogorov dynamics. *Surveys in Geophysics* **34**:181-207.
- Markonis, Y., and D. Koutsoyiannis. 2016. Scale-dependence of persistence in precipitation records. *Nature Climate Change*, 6 (4), 399-401.
- Nastos, P. T. 2011. Trends and variability of precipitation within the Mediterranean region, based on Global Precipitation Climatology Project (GPCP) and ground based datasets. Pages 67-74 *in* N. Lambrakis, G. Stournaras, and K. Katsanou, editors. *Advances in the Research of Aquatic Environment*. Springer Berlin Heidelberg.
- Norrant, C., and A. Douguédroit. 2006. Monthly and daily precipitation trends in the Mediterranean (1950–2000). *Theoretical and Applied Climatology* **83**:89-106.
- Partal, T., and E. Kahya. 2006. Trend analysis in Turkish precipitation data. *Hydrological Processes* **20**:2011-2026.
- Pelletier, J. D., and D. L. Turcotte. 1997. Long-range persistence in climatological and hydrological time series: analysis, modeling and application to drought hazard assessment. *Journal of Hydrology* **203**:198-208.
- Philandras, C. M., P. T. Nastos, J. Kapsomenakis, K. C. Douvis, G. Tselioudis, and C. S. Zerefos. 2011. Long term precipitation trends and variability within the Mediterranean region. *Nat. Hazards Earth Syst. Sci.* **11**:3235-3250.
- R Core Team. 2014. *R: A Language and Environment for Statistical Computing*.
- Rodrigo, F., and R. M. Trigo. 2007. Trends in daily rainfall in the Iberian Peninsula from 1951 to 2002. *International Journal of Climatology* **27**:513-529.
- Serrano, A., V. Mateos, and J. Garcia. 1999. Trend analysis of monthly precipitation over the Iberian Peninsula for the period 1921–1995. *Physics and Chemistry of the Earth, Part B: Hydrology, Oceans and Atmosphere* **24**:85-90.
- Solomon, S. 2007. *Climate change 2007-the physical science basis: Working group I contribution to the fourth assessment report of the IPCC*. Cambridge University Press.
- Stephenson, D. B., V. Pavan, and R. Bojariu. 2000. Is the North Atlantic Oscillation a random walk? *International Journal of Climatology* **20**:1-18.
- Stocker, T. F., D. Qin, G.-K. Plattner, M. Tignor, S. K. Allen, J. Boschung, A. Nauels, Y. Xia, V. Bex, and P. M. Midgley. 2013. *Climate change 2013: The physical science basis. Intergovernmental Panel on Climate Change, Working Group I Contribution to the IPCC Fifth Assessment Report (AR5)*(Cambridge Univ Press, New York).
- Tolika, K., C. Anagnostopoulou, P. Maheras, and H. Kutiel. 2007. Extreme precipitation related to circulation types for four case studies over the Eastern Mediterranean. *Advances in Geosciences* **12**:87-93.
- Tsekouras, G., and D. Koutsoyiannis. 2014. Stochastic analysis and simulation of hydrometeorological processes associated with wind and solar energy. *Renewable Energy* **63**:624-633.
- Tsonis, A., and P. Roebber. 2004. The architecture of the climate network. *Physica A: Statistical Mechanics and its Applications* **333**:497-504.
- Tyralis, H., and D. Koutsoyiannis. 2011. Simultaneous estimation of the parameters of the Hurst–Kolmogorov stochastic process. *Stochastic Environmental Research and Risk Assessment* **25**:21-33.
- Xoplaki, E., J. F. González-Rouco, J. Luterbacher, and H. Wanner. 2004. Wet season Mediterranean precipitation variability: influence of large-scale dynamics and trends. *Climate Dynamics* **23**:63-78.
- Xoplaki, E., J. Luterbacher, R. Burkard, I. Patrikas, and P. Maheras. 2000. Connection between the large-scale 500 hPa geopotential height fields and precipitation over Greece during wintertime. *Climate Research* **14**:129-146.
- Xu, Z., T. Gong, and J. Li. 2008. Decadal trend of climate in the Tibetan Plateau—regional temperature and precipitation. *Hydrological Processes* **22**:3056-3065.
- Zhai, Y., Y. Guo, J. Zhou, N. Guo, J. Wang, and Y. Teng. 2014. The spatio-temporal variability of annual precipitation and its local impact factors during 1724–2010 in Beijing, China. *Hydrological Processes* **28**:2192-2201.